Joint Beamforming Design and Power Splitting Optimization in IRS-Assisted SWIPT NOMA Networks

Zhendong Li, Wen Chen, *Senior Member, IEEE*, and Qingqing Wu, *Member, IEEE*

Abstract

This paper proposes a novel network framework of intelligent reflecting surface (IRS)-assisted simultaneous wireless information and power transfer (SWIPT) non-orthogonal multiple access (NOMA) networks, in which IRS is used to enhance the performance of NOMA and the wireless power transfer (WPT) efficiency of SWIPT. We formulate a problem of minimizing base station (BS) transmit power by jointly optimizing successive interference cancellation (SIC) decoding order, BS transmit beamforming vector, power splitting (PS) ratio and IRS phase shifts while taking into account the quality-of-service (QoS) requirement and energy harvested threshold of each user. The formulated problem is non-convex optimization problem, which is difficult to solve it directly. Hence, a two-stage algorithm is proposed to solve the above-mentioned problem by applying semidefinite relaxation (SDR) and Gaussian randomization. Specifically, after determining the SIC decoding order by designing the IRS phase shifts in the first stage, we alternately optimize the transmit beamforming vector, PS ratio, and IRS phase shifts to minimize the BS transmit power. Numerical results validate the effectiveness of our proposed optimization algorithm in reducing BS transmit power compared to other baseline algorithms. Meanwhile, the IRS-assisted SWIPT NOMA networks require lower BS transmit power than the non-IRS-assisted networks.

Index Terms

Intelligent reflecting surface (IRS), simultaneous wireless information and power transfer (SWIPT), non-orthogonal multiple access (NOMA), IRS phase shifts, power splitting ratio.

Z. Li and W. Chen are with the Department of Electronic Engineering, Shanghai Jiao Tong University, Shanghai 200240, China (e-mail: lizhendong@sjtu.edu.cn; wenchen@sjtu.edu.cn).

Q. Wu is with the State Key Laboratory of Internet of Things for Smart City, University of Macau, Macau, China (email: qingqingwu@um.edu.mo).

I. Introduction

With the vigorous development of emerging services such as the Internet of Things (IoT) and mobile Internet, the surge in wireless devices poses unprecedented challenges to beyond fifth-generation/sixth-generation (B5G/6G) communication systems in terms of massive connectivity, spectrum efficiency, energy management, and deployment costs [1]–[3]. In order to meet the massive connectivity of future networks and the higher service requirements of users, non-orthogonal multiple access (NOMA) technology has triggered extensive discussions in academia and industry. Unlike conventional orthogonal multiple access (OMA) [4], NOMA can support multiple users to share the same resources, e.g., time, frequency, coding, etc., so it can support massive connectivity of users. Specifically, taking an instance of NOMA in the power domain, the base station (BS) uses the same resource blocks to serve multiple users, which can greatly improve the spectrum efficiency to meet the users' communication requirements [5]–[8]. For power domain NOMA transmission in the downlink, superposition coding and successive interference cancellation (SIC) techniques are applied at the BS transmitter and at the users respectively [5], [9]. As such, users with stronger channel gains can remove co-channel interference caused by users with weaker channel gains before decoding [10].

In general, existing research on NOMA considers that the users' channel conditions differ greatly, i.e., there are one type of users near the BS, and the other type of users are at the edge of the BS. In this way, the BS will allocate more transmit power to users with poor channel conditions. The main reason for this consideration is that the large difference in channel conditions will greatly release the potential of NOMA [11]. More specifically, if the difference in user channel conditions is small, the transmission performance of NOMA is not much better than that of OMA. However, in practical scenarios, the difference in user channel conditions for the NOMA networks is not always very large. This is because the wireless channel is determined by the propagation environment, which is highly random and uncontrollable. Therefore, if the channel can be controlled and adjusted, the performance of NOMA transmission will be greatly enhanced.

In addition, considering the need to provide continuous information transmission and energy transmission for large-scale low-power and energy-constrained IoT devices, simultaneous wireless information and power transfer (SWIPT) technology has attracted great attention recently. By applying SWIPT, users can obtain information and energy at the same time, which brings

great convenience to the deployment of energy-constrained IoT devices [12], [13]. As one of the design schemes of practical SWIPT receivers, the power splitting (PS) scheme aims to split the signal received by the receiver into two different power streams with one part used to decode information and the other part used to harvest energy [14]. Based on the PS scheme, [15] proposed a novel integrated SWIPT receiver architecture to achieve miniaturization and energy saving of the receiver. However, for the conventional SWIPT system, the wireless power transfer (WPT) efficiency will decrease sharply as the distance increases due to severe propagation loss, which thus greatly limits the performance of the SWIPT system. If the channel conditions can be strengthened, the WPT efficiency and coverage will be improved.

Recently, intelligent reflecting surface (IRS) has been proposed as a promising cost-effective solution to control and adjust the wireless channel between transceivers [1], [16]–[18]. Furthermore, it can greatly improve the spectrum efficiency, energy efficiency, and coverage of the networks, while reducing networking costs [19], [20]. Therefore, it has received widespread attention from academia and industry [21] and has also been recognized as a key enabling for the future 6G ecosystem [22]. Specifically, IRS is composed of a large number of passive reflecting elements, which can be easily deployed on indoor walls or buildings. It can adjust the amplitude and phase of the incident signal, and realize the reconstruction of the wireless channel. Unlike conventional relays, IRS is a passive device, which only passively reflects the incident signal without signal processing, so it does not introduce additional noise [23], [24]. Unlike multiple-input multiple-output (MIMO), the required hardware cost and power consumption are much lower. These have greatly promoted the application of IRS in B5G/6G networks. Based on these significant advantages of IRS, the momentum of the IRS-assisted SWIPT NOMA networks in the IoT has been stimulated. First of all, IRS reconstructs the wireless channel to make the difference in channel conditions among users, thereby enhancing the performance of NOMA transmission. In addition, it can improve the efficiency of energy transmission of SWIPT system, and expand the network coverage. In short, IRS-enhanced wireless networks can meet the challenges of future B5G/6G networks in terms of massive connectivity, spectrum efficiency, energy management, and cost etc..

Recently, the application of IRS-assisted wireless networks in different scenarios and different technologies has continued to emerge, e.g., IRS-assisted massive MIMO [25]–[27], IRS-assisted mobile edge computing [28], IRS-assisted unmanned aerial vehicle (UAV) communication [29], [30] and IRS-assisted physical layer security [26], [31], [32] etc.. In addition, many scholars are

currently committed to the research of IRS-enhanced NOMA transmission [2], [33]–[38] and the research of IRS-assisted SWIPT technology [39]–[41]. For the research of IRS-enhanced NOMA transmission, Fu *et al.* jointly optimized the BS beamforming vector and the phase shift matrix of the IRS in the NOMA network to minimize the total transmit power [33]. In [35], Zuo *et al.* considered the NOMA network in the single-input single-output (SISO) scenario, with the goal of maximizing system throughput, jointly optimizing the decoding order, channel selection and the phase shift matrix of the IRS, so that the system throughput was improved. In [2], Ni *et al.* proposed a new framework for resource allocation in multi-cell IRS-assisted NOMA networks. They maximized achievable sum rate by jointly optimizing user connections, sub-channel allocation, power allocation, IRS phase shift design, and decoding order. In [38], Zhu *et al.* proposed an IRS-assisted downlink energy-efficient multiple-input single-output (MISO) transmission scheme, which greatly reduces the transmit power by optimizing the beamforming vector and the phase shift matrix of the IRS. Meanwhile, some progress has been made in the research on IRS-assisted SWIPT. In the IRS-assisted SWIPT networks, Wu *et al.* jointly optimized the active and passive beamforming vector to increase the weighted received power of information user (IU) and energy user (EU) [39]. At the same time, a novel algorithm was adopted in [40] to solve the problem of maximizing the weighted received power of IU and EU under the condition of satisfying all users' QoS. Pan *et al.* studied IRS-assisted MIMO SWIPT networks in [41], which optimized the weighted sum rate of information receivers (IRs) while meeting the energy requirements of energy receivers (ERs).

Although there have been many studies on IRS-assisted wireless communication networks. However, the B5G/6G network will be a more complex and changeable network. The massive connectivity, spectrum efficiency, energy management and deployment cost of the network will greatly stimulate our motivation to integrate IRS with NOMA and SWIPT in order to better satisfy the business requirements of users in IoT networks. As far as we know, the current research on IRS-assisted SWIPT NOMA networks is still in its infancy. In this paper, under the constraints of meeting the users' QoS requirements and energy harvested thresholds, we minimize the BS transmit power by jointly optimizing the SIC decoding order, the BS transmit beamforming vector, the user's received PS ratio, and the IRS reflecting phase shift coefficient. This problem is challenging mainly because the changes of wireless channel make the users' decoding order more complicated, and the BS transmit beamforming vector, PS ratio, and IRS phase shift coefficient are highly coupled. Therefore, it is necessary to design an effective algorithm for the

IRS-assisted SWIPT NOMA networks to minimize the BS transmit power.

Based on the above, the main contributions of this paper can be summarized as follows:

- We propose an IRS-assisted SWIPT NOMA network framework, in which multiple users can share the same resource blocks at the same time, and users can obtain energy while receiving information. In addition, IRS can adjust the channel to improve NOMA transmission performance and SWIPT WPT efficiency. We formulate an optimization problem that minimizes the BS transmit power with the constraints of users' QoS requirements and energy harvested threshold. This problem jointly optimizes the SIC decoding order, the BS transmit beamforming vector, the PS ratio, and the IRS phase shifts. Since the variables in the optimization problem are highly coupled, the solution of this problem is challenging.
- In order to solve the optimization problem mentioned above, we divide the problem into two stages. Specifically, in the first stage, an SIC decoding order determination algorithm is proposed based on the maximum combined channel strength. In the second stage, we divide the problem into two sub-problems according to the decoding order obtained in the first stage. First, given the IRS phase shifts, the BS transmit beamforming vector and PS ratio are jointly optimized by applying semidefinite relaxation (SDR), and it is proved that the SDR is tight. Furthermore, the IRS phase shift optimization problem is transformed into a feasibility-check problem, and it is solved by applying SDR and Gaussian randomization. Finally, the two sub-problems are iterated alternately until convergence.
- Through numerical simulation, we verified the effectiveness of the proposed joint SIC decoding order, BS transmit beamforming vector, PS ratio, and IRS phase shift optimization algorithm (JDBPR) compared with the baseline algorithm, i.e., it can significantly decrease the BS transmit power. For the IRS-assisted NOMA SWIPT networks, the BS transmit power is significantly lower than the networks without IRS assistance. Meanwhile, the more reflecting elements of the IRS, the smaller the required transmit power, which also means that we can reduce the transmit power on BS by increasing the number of IRS elements.

The remainder of this paper is organized as follows. Section II elaborates the system model and optimization problem formulation for the IRS-assisted SWIPT NOMA networks. Section III presents the proposed two-stage optimization algorithm for the formulated optimization problem. In Section IV, numerical results demonstrate that our algorithm has good convergence and effectiveness. Finally, the conclusion is given in Section V.

Notations: Scalars are denoted by lower-case letters, while vectors and matrices are represented

by bold lower-case letters and bold upper-case letters, respectively. $|x|$ denotes the absolute value of a complex-valued scalar x, and $\|\mathbf{x}\|$ denotes the Euclidean norm of a complex-valued vector $\mathbf{x}$. $diag(\mathbf{x})$ denotes a diagonal matrix whose diagonal elements are the corresponding elements in vector $\mathbf{x}$. For a square matrix $\mathbf{X}$, $\mathrm{Tr}(\mathbf{X})$, $\mathrm{Rank}(\mathbf{X})$, $\mathbf{X}^H$ and $\mathbf{X}_{m,n}$ denote its trace, rank, conjugate transpose and m,n-th entry, respectively, while $\mathbf{X} \succeq 0$ represents that $\mathbf{X}$ is a positive semidefinite matrix. Similarly, for a general matrix $\mathbf{A}$, $\mathrm{Tr}(\mathbf{A})$, $\mathrm{Rank}(\mathbf{A})$, $\mathbf{A}^H$ and $\mathbf{A}_{m,n}$ also denote its trace, rank, conjugate transpose and m,n-th entry, respectively. In addition, $\mathbb{C}^{M\times N}$ denotes the space of $M \times N$ complex matrices. $\mathbf{I}_N$ denotes an dentity matrix of size $N \times N$. j denotes the imaginary unit, i.e., $j^2 = -1$. Finally, the distribution of a circularly symmetric complex Gaussian (CSCG) random vector with mean μ and covariance matrix $\mathbf{C}$ is denoted by $\mathcal{CN}(\mu, \mathbf{C})$, and $\sim$ stands for 'distributed as'.

II. System model and problem formulation

A. System model

In this paper, we consider the downlink transmission in an IRS-assisted SWIPT NOMA network consisting of one BS, one IRS and K users. The set of users is denoted by $\mathcal{K} = \{1, 2, ..., K\}$. It can be assumed that the BS is equipped with $N > 1$ uniform linear array (ULA) antennas and each user is equipped with one antenna. The IRS consists of M ULA reflecting elements, denoted by $\mathcal{M} = \{1, 2, ..., M\}$. A smart controller is equipped at the IRS to coordinate its switching between two working modes [42]. Due to the high path loss, signals reflected by the IRS twice or more are negligible and can be ignored. We assume all channels are quasi-static flat-fading and the channel state information (CSI) of all channels is perfectly known at the BS.

The channel gains from the BS to IRS, from the IRS to k-th user, and from the BS to k-user are respectively represented by $\mathbf{G} \in \mathbb{C}^{M\times N}$, $\mathbf{h}_{r,k}^H \in \mathbb{C}^{1\times M}$ and $\mathbf{h}_{d,k}^H \in \mathbb{C}^{1\times N}$, $\forall k \in \mathcal{K}$. Let $\mathbf{\Theta} = \mathrm{diag}\left(\beta_1 e^{j\theta_1}, \beta_2 e^{j\theta_2}, ..., \beta_M e^{j\theta_M}\right) \in \mathbb{C}^{M\times M}$ denote the reflection coefficients matrix of the IRS, where $\beta_m \in [0, 1]$ and $\theta_m \in [0, 2\pi]$ denote the amplitude reflection coefficient and phase shift of the m-th reflecting element, respectively. In the deployment of actual scenarios, we usually consider that the reflecting element of the IRS is designed to maximize the reflected signal, so β_m= 1,$\forall m \in \mathcal{M}$. The wireless channel can be divided into three parts, namely, BS-IRS channel, IRS-user channel, BS-user channel. Although the channel between the BS and users may be blocked, the wireless channel still has a lot of scattering, thus we model the BS-user channel as Rayleigh fading and denote it as $\mathbf{g}_{d,k}^H \in \mathbb{C}^{1\times N}$. We assume that each element of $\mathbf{g}_{d,k}^H$

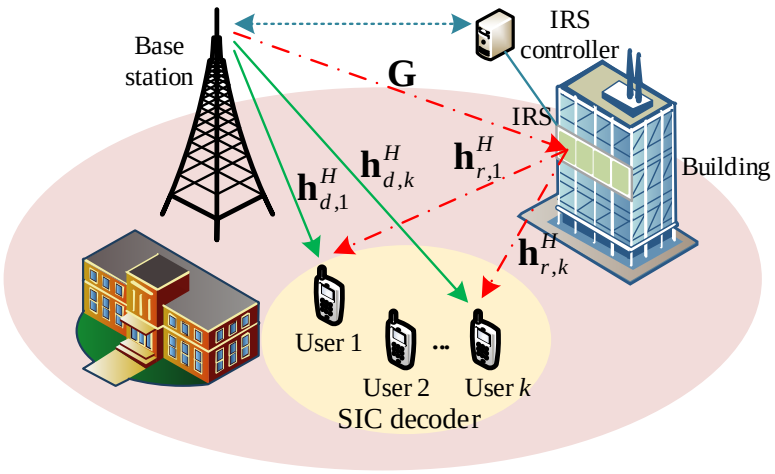

Fig. 1. The IRS-assisted SWIPT NOMA networks.

is independent and identically distributed (i.i.d.) CSCG random variable with zero mean and unit variance. Therefore, the channel gain of the BS-user can be expressed as

$$\mathbf{h}_{d,k}^H = \sqrt{C_0 \left(\frac{d_{d,k}}{D_0}\right)^{-\alpha}} \mathbf{g}_{d,k}^H, \tag{1}$$

where C_0 represents the path loss when the reference distance $D_0 = 1\,(\mathrm{m})$, $d_{d,k}$ is the distance from the BS to the k-th user, and α represents the path loss exponent.

In addition, for the BS-IRS channel and IRS-user channel, there are LoS components, thus we model them as Rician fading. The BS-IRS channel can be denoted by

$$\bar{\mathbf{G}} = \sqrt{\frac{\kappa}{1+\kappa}} \mathbf{G}^{\mathrm{LoS}} + \sqrt{\frac{1}{1+\kappa}} \mathbf{G}^{\mathrm{NLoS}}, \tag{2}$$

where κ is the Rician factor, $\mathbf{G}^{\mathrm{LoS}} \in \mathbb{C}^{M \times N}$ and $\mathbf{G}^{\mathrm{NLoS}} \in \mathbb{C}^{M \times N}$ are the line-of-sight (LoS) component and non-line-of-sight (NLoS) component, respectively. Each element of $\mathbf{G}^{\mathrm{NLoS}}$ is i.i.d. CSCG random variable with zero mean and unit variance. Similarly, the IRS-user channel can be expressed as

$$\bar{\mathbf{h}}_{r,k}^H = \sqrt{\frac{\vartheta}{1+\vartheta}} \mathbf{h}_{r,k}^{\mathrm{LoS}} + \sqrt{\frac{1}{1+\vartheta}} \mathbf{h}_{r,k}^{\mathrm{NLoS}}, \tag{3}$$

where ϑ is the Rician factor, $\mathbf{h}_{r,k}^{\mathrm{LoS}} \in \mathbb{C}^{1 \times M}$ and $\mathbf{h}_{r,k}^{\mathrm{NLoS}} \in \mathbb{C}^{1 \times M}$ are the LoS component and NLoS component, respectively. Each element of $\mathbf{h}_{r,k}^{\mathrm{NLoS}}$ is i.i.d. CSCG random variable with zero

mean and unit variance.

The LoS component is represented by the array response of ULA. The array response of N elements ULA can be expressed as

$$\mathbf{a}_N(\theta) = \left[1, e^{-j2\pi\frac{d}{\lambda}\sin\theta}, ..., e^{-j2\pi(N-1)\frac{d}{\lambda}\sin\theta}\right], \tag{4}$$

where θ represents the angle of arrival (AoA) or angle of departure (AoD) of the signal. Therefore, the LoS component $\mathbf{G}^{\mathrm{LoS}}$ can be given by

$$\mathbf{G}^{\mathrm{LoS}} = \mathbf{a}_M^H(\theta_{\mathrm{AoA},1})\,\mathbf{a}_N(\theta_{\mathrm{AoD},1}), \tag{5}$$

where $\theta_{\mathrm{AoA},1}$ is the AoA to the ULA at the IRS, and $\theta_{\mathrm{AoD},1}$ is the AoD from the ULA at the BS. Similarly, the LoS component $\mathbf{h}_{r,k}^{\mathrm{LoS}}$ can be expressed as

$$\mathbf{h}_{r,k}^{\mathrm{LoS}} = \mathbf{a}_M(\theta_{\mathrm{AoD},2}), \tag{6}$$

where $\theta_{\mathrm{AoD},2}$ is the AoD from the ULA at the IRS.

Therefore, the channel gain of BS-IRS and IRS-user can be expressed as

$$\mathbf{G} = \sqrt{C_0\left(\frac{d_{d,r}}{D_0}\right)^{-\beta}}\bar{\mathbf{G}}, \tag{7}$$

and

$$\mathbf{h}_{r,k}^H = \sqrt{C_0\left(\frac{d_{r,k}}{D_0}\right)^{-o}}\bar{\mathbf{h}}_{r,k}^H, \tag{8}$$

where $d_{d,r}$ and $d_{r,k}$ represent the distance from the BS to the IRS and the distance from the IRS to the k-th user, respectively. β and o respectively represent the path loss exponent from BS to IRS and IRS to the k-th user.

In this paper, we assume linear transmit precoding at BS, where each user is assigned with one dedicated information beam. Therefore, the complex baseband transmitted signal at BS can be expressed as

$$\mathbf{x} = \sum_{k=1}^{K}\mathbf{w}_k s_k, \forall k \in \mathcal{K}, \tag{9}$$

where s_k denotes the transmission data symbol for the k-th user, and $\mathbf{w}_k \in \mathbb{C}^{N\times 1}$ represents the corresponding beamforming vector. We assume that $s_k, \forall k \in \mathcal{K}$ is i.i.d. CSCG random variables with zero mean and unit variance, denoted by $s_k \sim \mathcal{CN}(0,1), \forall k \in \mathcal{K}$.

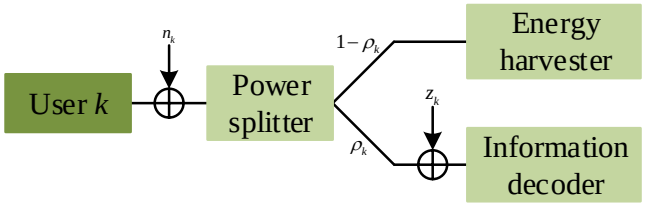

Fig. 2. The PS receiver architecture.

The received signal at the k-th user from both the BS-user link and BS-IRS-user link can be expressed as

$$y_k = \left(\mathbf{h}_{r,k}^H \mathbf{\Theta} \mathbf{G} + \mathbf{h}_{d,k}^H\right) \sum_{j=1}^{K} \mathbf{w}_j s_j + n_k, \forall k \in \mathcal{K}, \tag{10}$$

where $n_k \sim \mathcal{CN}\left(0, \sigma_k^2\right)$ denotes the antenna noise at the k-th user.

In addition, we consider that each user applies PS scheme to coordinate the processes of information decoding and energy harvesting from the received signal [14]. The received signal at each user is split to the information decoder (ID) and the energy harvester (EH) by a power splitter. For the k-th user, it divides $\rho_k \left(0 \leq \rho_k \leq 1\right)$ portion of the signal power to the ID, remaining $1-\rho_k$ portion of the signal power to the EH. Therefore, the signal split to the ID for k-th user can be given by

$$y_k^{\mathrm{ID}} = \sqrt{\rho_k} \left(\left(\mathbf{h}_{r,k}^H \mathbf{\Theta} \mathbf{G} + \mathbf{h}_{d,k}^H\right) \sum_{j=1}^{K} \mathbf{w}_j s_j + n_k \right) + z_k, \forall k \in \mathcal{K}, \tag{11}$$

where $z_k \sim \mathcal{CN}\left(0, \delta_k^2\right)$ is the additional noise introduced by the ID at the k-th user.

Since we consider NOMA transmission, the SIC decoding order is very important, which is determined by the channel conditions. Unlike the general NOMA communication system, the combination of IRS and NOMA makes the channel more complicated, because the channel gain may change due to the change of the IRS phase shift matrix. Let $s\left(k\right)$ denote the decoding order for the k-th user. Then, $s\left(k\right) = i$ denotes that the k-th user is the i-th signal to be decoded at the receiver. Accordingly, the signal to interference plus noise ratio (SINR) of the k-th user can

be expressed as

$$\mathrm{SINR}_k = \frac{\rho_k \left| \left(\mathbf{h}_{r,k}^H \mathbf{\Theta} \mathbf{G} + \mathbf{h}_{d,k}^H \right) \mathbf{w}_k \right|^2}{\rho_k \sum\limits_{s(j)>s(k)} \left| \left(\mathbf{h}_{r,k}^H \mathbf{\Theta} \mathbf{G} + \mathbf{h}_{d,k}^H \right) \mathbf{w}_j \right|^2 + \rho_k \sigma_k^2 + \delta_k^2}. \tag{12}$$

It is assumed that $s(k) \leq s\left(\bar{k}\right)$, the SINR of the $\bar{k}$-th user decoding information signal of the k-th user can be given by

$$\mathrm{SINR}_{\bar{k}\to k} = \frac{\rho_k \left| \left(\mathbf{h}_{r,\bar{k}}^H \mathbf{\Theta} \mathbf{G} + \mathbf{h}_{d,\bar{k}}^H \right) \mathbf{w}_k \right|^2}{\rho_k \sum\limits_{s(j)>s(k)} \left| \left(\mathbf{h}_{r,\bar{k}}^H \mathbf{\Theta} \mathbf{G} + \mathbf{h}_{d,\bar{k}}^H \right) \mathbf{w}_j \right|^2 + \rho_k \sigma_k^2 + \delta_k^2}. \tag{13}$$

In order to ensure that the $\bar{k}$-th user can decode the information of the k-th user with the decoding order $s(k) \leq s\left(\bar{k}\right)$, the SIC decoding condition $\mathrm{SINR}_{\bar{k}\to k} > \mathrm{SINR}_k$ should be satisfied [43]. For example, supposing the decoding order of the three users is $s(k) = i, i = 1, 2, 3$. Therefore, the SIC decoding conditions at user 2 and user 3 should satisfy the following conditions: $\mathrm{SINR}_{2\to 1} > \mathrm{SINR}_1$, $\mathrm{SINR}_{3\to 1} > \mathrm{SINR}_1$ and $\mathrm{SINR}_{3\to 2} > \mathrm{SINR}_2$. In addition, the signal split to the EH for the k-th user can be expressed as

$$y_k^{\mathrm{EH}} = \sqrt{1-\rho_k} \left(\left(\mathbf{h}_{r,k}^H \mathbf{\Theta} \mathbf{G} + \mathbf{h}_{d,k}^H \right) \sum_{j=1}^{K} \mathbf{w}_j s_j + n_k \right), \tag{14}$$

Then, the harvested power by the EH for the k-th user can be given by

$$E_k = \eta_k \left(1-\rho_k\right) \left(\sum_{j=1}^{K} \left| \left(\mathbf{h}_{r,k}^H \mathbf{\Theta} \mathbf{G} + \mathbf{h}_{d,k}^H \right) \mathbf{w}_j \right|^2 + \sigma_k^2 \right), \tag{15}$$

where $\eta_k \in (0, 1]$ denotes the energy conversion efficiency at EH of the k-th user.

B. Problem formulation for the IRS-assisted SWIPT NOMA system

Let $\mathbf{w} = [\mathbf{w}_1, ..., \mathbf{w}_K] \in \mathbb{C}^{N\times K}$, $\boldsymbol{\rho} = [\rho_1, ..., \rho_K]$, $\mathbf{s} = [s(1), ..., s(K)]$. In this paper, we aim to minimize the BS transmit power by jointly designing SIC decoding order, BS transmit beamforming vector, received PS ratio and IRS phase shift matrix. Accordingly, the problem can be formulated as the E.q. (16). Constraint (16b) guarantees the QoS requirement of the k-th user with the SINR threshold γ_k. Meanwhile, constraint (16c) ensures SIC decoding conditions. In addition, constraint (16d) requires that the energy harvested of the k-th user needs to reach a threshold e_k. Considering that each user should have non-zero SINR threshold and energy

harvested threshold, i.e., $\gamma_k > 0$ and $e_k > 0$, the received PS ratio of the k-th user should satisfy constraint (16e). (16f) is the condition that IRS phase shifts should meet. Ω in constraint (16g) is the combination set of all possible SIC decoding orders.

$$(\text{P1}) \qquad \min_{\mathbf{w},\boldsymbol{\Theta},\boldsymbol{\rho},\mathbf{s}} \sum_{k=1}^{K} \|\mathbf{w}_k\|^2, \tag{16a}$$

$$\text{s.t.} \qquad \frac{\rho_k \left| \left(\mathbf{h}_{r,k}^H \boldsymbol{\Theta} \mathbf{G} + \mathbf{h}_{d,k}^H\right) \mathbf{w}_k \right|^2}{\rho_k \sum\limits_{s(j)>s(k)} \left| \left(\mathbf{h}_{r,k}^H \boldsymbol{\Theta} \mathbf{G} + \mathbf{h}_{d,k}^H\right) \mathbf{w}_j \right|^2 + \rho_k \sigma_k^2 + \delta_k^2} \geq \gamma_k, \tag{16b}$$

$$\mathrm{SINR}_{\bar{k}\to k} \geq \mathrm{SINR}_k, \ \text{if} \ s\left(\bar{k}\right) \geq s\left(k\right), \tag{16c}$$

$$\eta_k \left(1-\rho_k\right) \left(\sum_{j=1}^{K} \left| \left(\mathbf{h}_{r,k}^H \boldsymbol{\Theta} \mathbf{G} + \mathbf{h}_{d,k}^H\right) \mathbf{w}_j \right|^2 + \sigma_k^2 \right) \geq e_k, \tag{16d}$$

$$0 < \rho_k < 1, \forall k \in \mathcal{K}, \tag{16e}$$

$$0 \leq \theta_m \leq 2\pi, \forall m \in \mathcal{M}, \tag{16f}$$

$$s \in \Omega. \tag{16g}$$

It can be seen that the problem (P1) is a non-convex optimization problem due to the following reasons. Firstly, the beamforming vector $\mathbf{w}$, the receive PS ratio $\boldsymbol{\rho}$ and the IRS phase shift matrix $\boldsymbol{\Theta}$ are highly coupled. In addition, the phase shift is expressed in exponential form. Finally, the SIC decoding orders $\mathbf{s}$ are determined by the IRS phase shifts, thus the SIC decoding order $\mathbf{s}$ and the IRS phase shifts are also coupled. Therefore, it is challenging to directly solve this problem.

C. Feasibility analysis of the problem

It can be seen that the problem (P1) has four blocks of optimization variables $\mathbf{w}, \boldsymbol{\Theta}, \boldsymbol{\rho}, \mathbf{s}$, and we analyze the feasibility of the problem under the conditions of $\gamma_k > 0$ and $e_k > 0$.

Lemma 1: The problem (P1) is feasible if and only if the problem (P1.1) is feasible.

$$\text{(P1.1)} \quad \text{find} \quad \mathbf{w}_k, \mathbf{\Theta}, \rho_k, \tag{17a}$$

$$\text{s.t.} \quad \frac{\rho_k \left| \left(\mathbf{h}_{r,k}^H \mathbf{\Theta} \mathbf{G} + \mathbf{h}_{d,k}^H \right) \mathbf{w}_k \right|^2}{\rho_k \sum\limits_{s(j)>s(k)} \left| \left(\mathbf{h}_{r,k}^H \mathbf{\Theta} \mathbf{G} + \mathbf{h}_{d,k}^H \right) \mathbf{w}_j \right|^2 + \rho_k \sigma_k^2 + \delta_k^2} \geq \gamma_k, \tag{17b}$$

$$0 < \rho_k < 1, \forall k \in \mathcal{K}, \tag{17c}$$

$$0 \leq \theta_m \leq 2\pi, \forall m \in \mathcal{M}. \tag{17d}$$

Proof: For the optimization variable decoding order $\mathbf{s}$ in the problem (P1), for any given decoding order $\mathbf{s}$, the constraint (16c) is automatically satisfied. So this constraint has no effect on the feasibility of the problem (P1). In addition, we can see that due to the additional energy harvested constraint (16d) in the problem (P1), if the problem (P1.1) is not feasible, then the problem (P1) must be infeasible. We assume that the problem (P1.1) is feasible, and one of its feasible solutions is $\mathbf{w}_k, \mathbf{\Theta}, \rho_k$. It can be seen that another solution $\tau \mathbf{w}_k, \mathbf{\Theta}, \rho_k, \tau > 1$ for the first constraint in problem (P1.1) can be expressed as

$$\begin{aligned}
&\frac{\rho_k \left| \left(\mathbf{h}_{r,k}^H \mathbf{\Theta} \mathbf{G} + \mathbf{h}_{d,k}^H \right) \tau \mathbf{w}_k \right|^2}{\rho_k \sum\limits_{s(j)>s(k)} \left| \left(\mathbf{h}_{r,k}^H \mathbf{\Theta} \mathbf{G} + \mathbf{h}_{d,k}^H \right) \tau \mathbf{w}_j \right|^2 + \rho_k \sigma_k^2 + \delta_k^2} = \frac{\tau^2 \rho_k \left| \left(\mathbf{h}_{r,k}^H \mathbf{\Theta} \mathbf{G} + \mathbf{h}_{d,k}^H \right) \mathbf{w}_k \right|^2}{\tau^2 \rho_k \sum\limits_{s(j)>s(k)} \left| \left(\mathbf{h}_{r,k}^H \mathbf{\Theta} \mathbf{G} + \mathbf{h}_{d,k}^H \right) \mathbf{w}_j \right|^2 + \rho_k \sigma_k^2 + \delta_k^2} \\
&= \frac{\rho_k \left| \left(\mathbf{h}_{r,k}^H \mathbf{\Theta} \mathbf{G} + \mathbf{h}_{d,k}^H \right) \mathbf{w}_k \right|^2}{\rho_k \sum\limits_{s(j)>s(k)} \left| \left(\mathbf{h}_{r,k}^H \mathbf{\Theta} \mathbf{G} + \mathbf{h}_{d,k}^H \right) \mathbf{w}_j \right|^2 + \frac{\rho_k \sigma_k^2}{\tau^2} + \frac{\delta_k^2}{\tau^2}} \geq \frac{\rho_k \left| \left(\mathbf{h}_{r,k}^H \mathbf{\Theta} \mathbf{G} + \mathbf{h}_{d,k}^H \right) \mathbf{w}_k \right|^2}{\rho_k \sum\limits_{s(j)>s(k)} \left| \left(\mathbf{h}_{r,k}^H \mathbf{\Theta} \mathbf{G} + \mathbf{h}_{d,k}^H \right) \mathbf{w}_j \right|^2 + \rho_k \sigma_k^2 + \delta_k^2} \\
&\geq \gamma_k.
\end{aligned} \tag{18}$$

That is, another solution $\tau \mathbf{w}_k, \mathbf{\Theta}, \rho_k, \tau > 1$ is also feasible for the problem (P1.1). Since $\tau > 0$, there must be a sufficiently large τ so that $\tau \mathbf{w}_k, \mathbf{\Theta}, \rho_k$ satisfies the energy constraint of problem (P1), i.e., it is feasible for problem (P1). The proof of **Lemma 1** is completed.

Lemma 1 shows that the feasibility of the problem (P1) depends on the QoS requirement constraint, not the energy harvested threshold constraint. The following lemma further simplifies the feasibility verification of the problem (P1.1).

Lemma 2: The problem (P1.1) is feasible if and only if the problem (P1.2) is feasible.

$$\text{(P1.2)} \quad \text{find} \quad \mathbf{w}_k, \mathbf{\Theta}, \tag{19a}$$

$$\text{s.t.} \quad \frac{\rho_k \left| \left(\mathbf{h}_{r,k}^H \mathbf{\Theta} \mathbf{G} + \mathbf{h}_{d,k}^H\right) \mathbf{w}_k \right|^2}{\rho_k \sum\limits_{s(j)>s(k)} \left| \left(\mathbf{h}_{r,k}^H \mathbf{\Theta} \mathbf{G} + \mathbf{h}_{d,k}^H\right) \mathbf{w}_j \right|^2 + \rho_k \sigma_k^2 + \delta_k^2} \geq \gamma_k, \tag{19b}$$

$$0 \leq \theta_m \leq 2\pi, \forall m \in \mathcal{M}. \tag{19c}$$

Proof: We assume that the problem (P1.2) is feasible. Let $\mathbf{w}_k, \mathbf{\Theta}$ denote the feasible solution of the problem (P1.2). For any given $0 < \rho_k < 1$, the feasible solution $\hat{\mathbf{w}}_k = \frac{\mathbf{w}_k}{\sqrt{\rho_k}}, \hat{\mathbf{\Theta}} = \mathbf{\Theta}, \hat{\rho}_k = \rho_k, \forall k$ of the problem (P1.1) satisfies the first constraint, which can be expressed as

$$\begin{aligned} &\frac{\hat{\rho}_k \left| \left(\mathbf{h}_{r,k}^H \hat{\mathbf{\Theta}} \mathbf{G} + \mathbf{h}_{d,k}^H\right) \hat{\mathbf{w}}_k \right|^2}{\hat{\rho}_k \sum\limits_{s(j)>s(k)} \left| \left(\mathbf{h}_{r,k}^H \hat{\mathbf{\Theta}} \mathbf{G} + \mathbf{h}_{d,k}^H\right) \hat{\mathbf{w}}_j \right|^2 + \hat{\rho}_k \sigma_k^2 + \delta_k^2} = \frac{\left| \left(\mathbf{h}_{r,k}^H \mathbf{\Theta} \mathbf{G} + \mathbf{h}_{d,k}^H\right) \mathbf{w}_k \right|^2}{\sum\limits_{s(j)>s(k)} \left| \left(\mathbf{h}_{r,k}^H \mathbf{\Theta} \mathbf{G} + \mathbf{h}_{d,k}^H\right) \mathbf{w}_j \right|^2 + \rho_k \sigma_k^2 + \delta_k^2} \\ &\geq \frac{\left| \left(\mathbf{h}_{r,k}^H \mathbf{\Theta} \mathbf{G} + \mathbf{h}_{d,k}^H\right) \mathbf{w}_k \right|^2}{\sum\limits_{s(j)>s(k)} \left| \left(\mathbf{h}_{r,k}^H \mathbf{\Theta} \mathbf{G} + \mathbf{h}_{d,k}^H\right) \mathbf{w}_j \right|^2 + \sigma_k^2 + \delta_k^2} \geq \gamma_k, \forall k. \end{aligned} \tag{20}$$

It can be seen that if the problem (P1.2) is feasible, then the problem (P1.1) will feasible as well and vice versa. We can complete the proof by contradiction.

We consider that the problem (P1.2) is not feasible, and suppose the feasible solution of the problem (P1.1) is determined by the following relationship

$$\begin{aligned} \gamma_k &\leq \frac{\rho_k \left| \left(\mathbf{h}_{r,k}^H \mathbf{\Theta} \mathbf{G} + \mathbf{h}_{d,k}^H\right) \mathbf{w}_k \right|^2}{\rho_k \sum\limits_{s(j)>s(k)} \left| \left(\mathbf{h}_{r,k}^H \mathbf{\Theta} \mathbf{G} + \mathbf{h}_{d,k}^H\right) \mathbf{w}_j \right|^2 + \rho_k \sigma_k^2 + \delta_k^2} = \frac{\left| \left(\mathbf{h}_{r,k}^H \mathbf{\Theta} \mathbf{G} + \mathbf{h}_{d,k}^H\right) \mathbf{w}_k \right|^2}{\sum\limits_{s(j)>s(k)} \left| \left(\mathbf{h}_{r,k}^H \mathbf{\Theta} \mathbf{G} + \mathbf{h}_{d,k}^H\right) \mathbf{w}_j \right|^2 + \sigma_k^2 + \frac{\delta_k^2}{\rho_k}} \\ &< \frac{\left| \left(\mathbf{h}_{r,k}^H \mathbf{\Theta} \mathbf{G} + \mathbf{h}_{d,k}^H\right) \mathbf{w}_k \right|^2}{\sum\limits_{s(j)>s(k)} \left| \left(\mathbf{h}_{r,k}^H \mathbf{\Theta} \mathbf{G} + \mathbf{h}_{d,k}^H\right) \mathbf{w}_j \right|^2 + \sigma_k^2 + \delta_k^2}, \forall k. \end{aligned} \tag{21}$$

It can be seen that the feasible solution $\mathbf{w}_k, \mathbf{\Theta}, \rho_k$ of the problem (P1.1) is also feasible for the problem (P1.2), which contradicts the infeasibility of the problem (P1.2). **Lemma 2** is proved.

Through **Lemma 1** and **Lemma 2**, we can find that the feasible conditions of the problem (P1) and the feasible conditions of the problem (P1.2) are the same. The feasibility conditions of the problem (P1.2) have been explained in [16]. Thus there is the following proposition.

Proposition 1: If $\text{Rank}\left(\mathbf{G}^H \mathbf{H}_r + \mathbf{H}_d\right) = K$ is satisfied, where $\mathbf{H}_r = [\mathbf{h}_{r,1}, \mathbf{h}_{r,2}, ..., \mathbf{h}_{r,K}] \in$

$\mathbb{C}^{M\times K}$, $\mathbf{H}_d = [\mathbf{h}_{d,1}, \mathbf{h}_{d,2}, ..., \mathbf{h}_{d,K}] \in \mathbb{C}^{N\times K}$, then the problem (P1.2) is feasible for the SINR target of a limited number of users.

Therefore, the problem (P1) of a given QoS requirement constraint and energy harvested threshold constraint can be simplified to a problem (P1.2) of checking whether the SINR satisfies the condition. The feasibility condition is given in **Proposition 1**. Without loss of generality, we assume that the problem below is feasible.

III. The proposed two-stage optimization algorithm for the IRS-assisted SWIPT NOMA networks

In this section, we propose a two-stage optimization algorithm to solve the problem (P1). The problem (P1) is decoupled into two stages. Firstly, an SIC decoding order determination algorithm based on combined channel strength is proposed. Then, for the given SIC decoding order, the beamforming vector, PS ratio and IRS phase shift matrix are alternately optimized. Given the IRS phase shift matrix, the beamforming vector and PS ratio optimization are solved by SDR. Then the IRS phase shift optimization is also solved when the beamforming vector and PS ratio are given.

A. SIC decoding order determination algorithm

In this subsection, the SIC decoding order determination algorithm based on the combined channel gains is proposed. In this paper, the decoding order is not only determined by the direct channel gain from the BS to the ground user, but by the combined channel gain from the BS to each user. The change of the IRS phase shift matrix will influence the strength of the combined channel. Since the same phase shift is different for all users, the combined channel gain of different users cannot be maximized at the same time. So we maximize the sum of the combined channel gains of all users, which can be expressed as follows,

$$\text{(P2)} \qquad \max_{\mathbf{\Theta}} \sum_{k=1}^{K} \left\| \mathbf{h}_{r,k}^H \mathbf{\Theta} \mathbf{G} + \mathbf{h}_{d,k}^H \right\|^2, \tag{22a}$$

$$\text{s.t.} \qquad 0 \le \theta_m \le 2\pi, \forall m \in \mathcal{M}, \tag{22b}$$

where $\mathbf{\Theta} = \text{diag}\left(e^{j\theta_1}, e^{j\theta_2}, ..., e^{j\theta_M}\right)$. Let $u_m = e^{j\theta_m}, \forall m \in \mathcal{M}$, $\mathbf{u} = [u_1, u_2, ..., u_M]^H \in \mathbb{C}^{M\times 1}$. Then the constraint on θ_m is equivalent to $|u_m| = 1, \forall m \in \mathcal{M}$. Let $\mathbf{a}_k = \text{diag}\left(\mathbf{h}_{r,k}^H\right) \mathbf{G} \in \mathbb{C}^{M\times N}$,

then $\left\|\mathbf{h}_{r,k}^H\mathbf{\Theta}\mathbf{G}+\mathbf{h}_{d,k}^H\right\|^2$ can be written as $\left\|\mathbf{u}^H\mathbf{a}_k+\mathbf{h}_{d,k}^H\right\|^2$. We introduce auxiliary variables as follows,

$$\mathbf{R}_k=\begin{bmatrix}\mathbf{a}_k\mathbf{a}_k^H & \mathbf{a}_k\mathbf{h}_{d,k}\\ \mathbf{h}_{d,k}^H\mathbf{a}_k^H & 0\end{bmatrix},\bar{\mathbf{u}}=\begin{bmatrix}\mathbf{u}\\ 1\end{bmatrix}. \tag{23}$$

Therefore, $\left\|\mathbf{u}^H\mathbf{a}_k+\mathbf{h}_{d,k}^H\right\|^2$ can be further expressed as $\bar{\mathbf{u}}^H\mathbf{R}_k\bar{\mathbf{u}}+\left\|\mathbf{h}_{d,k}^H\right\|^2$. Since $\bar{\mathbf{u}}^H\mathbf{R}_k\bar{\mathbf{u}}=\mathrm{Tr}\left(\mathbf{R}_k\bar{\mathbf{u}}\bar{\mathbf{u}}^H\right)$, we define $\mathbf{U}=\bar{\mathbf{u}}\bar{\mathbf{u}}^H$, where $\mathbf{U}\succeq 0$ and $\mathrm{Rank}\left(\mathbf{U}\right)=1$. Since the rank-one constraint is non-convex, we use SDR to relax this constraint first, and the problem (P2) can be transformed into

$$\text{(P2.1)}\qquad \max_{\mathbf{U}}\sum_{k=1}^{K}\left(\mathrm{Tr}\left(\mathbf{R}_k\mathbf{U}\right)+\left\|\mathbf{h}_{d,k}^H\right\|^2\right), \tag{24a}$$

$$\text{s.t.}\qquad \mathbf{U}_{m,m}=1, m=1,2,...,M+1, \tag{24b}$$

$$\mathbf{U}\succeq 0. \tag{24c}$$

The above problem (P2.1) is a standard semidefinite programming (SDP) problem, which can be solved by using CVX toolbox [44]. The problem (P2.1) is equivalent to the problem (P2) if and only if the optimal solution $\mathbf{U}^*$ of the problem (P2.1) is a rank-one matrix. However, under normal circumstances, the problem (P2.1) generally does not produce a rank-one solution, i.e., $\mathrm{Rank}\left(\mathbf{U}\right)\neq 1$. The optimal solution of problem (P2.1) is only the upper bound of problem (P2), so it is necessary to reconstruct the high-rank solution obtained from problem (P2.1) into a rank-one solution. In this paper, we use Gaussian randomization to reduce the rank of high-rank solution. Since $\mathrm{Rank}\left(\mathbf{U}\right)\neq 1$, the eigenvalue decomposition of $\mathbf{U}$ can be expressed as

$$\mathbf{U}=\mathbf{V}\mathbf{\Sigma}\mathbf{V}^H, \tag{25}$$

where $\mathbf{V}=[e_1,e_2,...,e_{M+1}]$ is the identity matrix of the eigenvector, and $\mathbf{\Sigma}=\mathrm{diag}\left(\lambda_1,\lambda_2,...,\lambda_{M+1}\right)$ is the diagonal matrix of the eigenvalue. Next, we generate two independent zero-mean normal distribution random vectors $\alpha\in\mathbb{R}^{(M+1)\times 1}$, $\beta\in\mathbb{R}^{(M+1)\times 1}$ and covariance matrix $\frac{1}{2}\mathbf{I}_{M+1}$. Let T be the maximum generation of candidate random variables. The Gaussian random vector of the t-th generation can be expressed as

$$\mathbf{r}_t=\alpha+\beta\sqrt{-1}, t=1,2,...,T. \tag{26}$$

Based on the obtained Gaussian random vector $\mathbf{r}_t \sim \mathcal{CN}(\mathbf{0}, \mathbf{I}_{M+1})$, we can obtain the suboptimal solution of the problem (P2.1), which can be expressed as

$$\bar{\mathbf{u}}_t = \mathbf{U}\mathbf{\Sigma}^{1/2}\mathbf{r}_t, t = 1, 2, ..., T. \tag{27}$$

Therefore, the candidate reflection matrix can be expressed as

$$\mathbf{\Theta}_t = \mathrm{diag}\left(e^{j \arg\left(\frac{\bar{\mathbf{u}}_t[m]}{\bar{\mathbf{u}}_t[M+1]}\right)} \middle| \forall m \in \mathcal{M} \right), \tag{28}$$

where $\bar{\mathbf{u}}_t[m]$ represents the m-th reflective element of $\bar{\mathbf{u}}_t$. According to the obtained candidate reflection matrix set $\{\mathbf{\Theta}_t | \, t = 1, 2, ..., T\}$, we can obtain the one that maximizes the combined channel gain of all users, i.e.,

$$t^* = \arg\max_t \sum_{k=1}^{K} \left\| \mathbf{h}_{r,k}^H \mathbf{\Theta} \mathbf{G} + \mathbf{h}_{d,k}^H \right\|^2. \tag{29}$$

It has been verified that SDR technique followed by such randomization scheme can guarantee at least a $\pi/4$-approximation of the optimal objective value of the problem (P2) [16]. The proposed SIC decoding order determination (SDOD) algorithm is summarized in **Algorithm 1**.

Algorithm 1 The **S**IC **D**ecoding **O**rder **D**etermination (SDOD) Algorithm

1: Initialize the maximum generation of candidate random variables T, solve the SDP problem (P2.1) and obtain an optimal solution $\mathbf{U}^*$.
2: **if** $\mathrm{Rank}\,(\mathbf{U}^*) = 1$ **then**
3: Calculate the eigenvalue λ and eigenvector $\mathbf{v}$ of $\mathbf{U}^*$.
4: Calculate $\mathbf{\Theta}^* = \mathrm{diag}\left(\sqrt{\lambda}\mathbf{v}\right)$.
5: **else**
6: The eigenvalue decomposition is obtained by Eq. (25).
7: **for** $t = 1, 2, ..., T$ **do**
8: Obtain the random vector $\mathbf{r}_t$ by using (26).
9: Obatin the candidate reflection coefficients matrix $\mathbf{\Theta}_t$ of IRS by using Eq. (28).
10: **end for**
11: Obtain the optimal reflection coefficients matrix $\mathbf{\Theta}^* = \mathbf{\Theta}_{t^*}$ of IRS, where t^* can be obtained by using Eq. (29).
12: **end if**
13: According to $\mathbf{\Theta}^*$, calculate the combined channel gain $\left\| \mathbf{h}_{r,k}^H \mathbf{\Theta}^* \mathbf{G} + \mathbf{h}_{d,k}^H \right\|^2$, and then arrange them in ascending order.
14: **return** the SIC decoding order $\mathbf{s}$.

B. Joint beamforming vector and PS ratio optimization

Constraint (16c) in the problem (P1) can be transformed into $\left\|\mathbf{h}_{r,\bar{k}}^H\mathbf{\Theta}\mathbf{G}+\mathbf{h}_{d,\bar{k}}^H\right\|^2-\left\|\mathbf{h}_{r,k}^H\mathbf{\Theta}\mathbf{G}+\mathbf{h}_{d,k}^H\right\|^2\geq 0, \bar{k}\geq k$, thus this constraint is only related to the IRS phase shift matrix.

We apply the SIC decoding order determination algorithm and fix the IRS phase shift matrix. Meanwhile, let $\mathbf{H}_k=\mathbf{h}_{r,k}^H\mathbf{\Theta}\mathbf{G}+\mathbf{h}_{d,k}^H\in\mathbb{C}^{1\times N}$. The problem (P1) can be transformed into the problem (P3), which can be expressed as

$$
\begin{aligned}
(\text{P3}) \quad & \min_{\mathbf{w},\boldsymbol{\rho}} \sum_{k=1}^{K}\left\|\mathbf{w}_k\right\|^2, && \text{(30a)}\\
\text{s.t.} \quad & \frac{\rho_k\left|\mathbf{H}_k\mathbf{w}_k\right|^2}{\rho_k\sum\limits_{s(j)>s(k)}\left|\mathbf{H}_k\mathbf{w}_j\right|^2+\rho_k\sigma_k^2+\delta_k^2}\geq\gamma_k, && \text{(30b)}\\
& \eta_k\left(1-\rho_k\right)\left(\sum_{j=1}^{K}\left|\mathbf{H}_k\mathbf{w}_j\right|^2+\sigma_k^2\right)\geq e_k, && \text{(30c)}\\
& 0<\rho_k<1, \forall k\in\mathcal{K}. && \text{(30d)}
\end{aligned}
$$

We apply SDR to solve the problem (P3). Define $\mathbf{W}_k{=}\mathbf{w}_k\mathbf{w}_k^H\in\mathbb{C}^{N\times N}, \forall k\in\mathcal{K}$, where $\mathbf{W}_k$ satisfies $\mathrm{Rank}\left(\mathbf{W}_k\right)\leq 1, \forall k\in\mathcal{K}$. We first ignore the rank-one constraint, the problem (P3) can be transformed into the problem (P3.1), which can be expressed as

$$
\begin{aligned}
(\text{P3.1}) \quad & \min_{\mathbf{W},\boldsymbol{\rho}} \sum_{k=1}^{K}\mathrm{Tr}\left(\mathbf{W}_k\right), && \text{(31a)}\\
\text{s.t.} \quad & \frac{\rho_k\mathbf{H}_k\mathbf{W}_k\mathbf{H}_k^H}{\rho_k\sum\limits_{s(j)>s(k)}\mathbf{H}_k\mathbf{W}_j\mathbf{H}_k^H+\rho_k\sigma_k^2+\delta_k^2}\geq\gamma_k, && \text{(31b)}\\
& \eta_k\left(1-\rho_k\right)\left(\sum_{j=1}^{K}\mathbf{H}_k\mathbf{W}_j\mathbf{H}_k^H+\sigma_k^2\right)\geq e_k, && \text{(31c)}\\
& \mathbf{W}_k\succeq 0, && \text{(31d)}\\
& 0<\rho_k<1, \forall k\in\mathcal{K}. && \text{(31e)}
\end{aligned}
$$

The problem (P3.1) is still a non-convex optimization problem. Due to the coupling of the transmit beamforming vector and PS ratio in the constraint, we decouple the two blocks of optimization variables to convert the problem (P3.1) into a convex problem (P3.2), which can

be expressed as follows,

$$(\text{P3.2}) \quad \min_{\mathbf{W},\boldsymbol{\rho}} \quad \sum_{k=1}^{K} \text{Tr}\left(\mathbf{W}_k\right), \tag{32a}$$

$$\text{s.t.} \quad \frac{\mathbf{H}_k \mathbf{W}_k \mathbf{H}_k^H}{\gamma_k} - \sum_{\pi(j)>\pi(k)} \mathbf{H}_k \mathbf{W}_j \mathbf{H}_k^H \geq \sigma_k^2 + \frac{\delta_k^2}{\rho_k}, \tag{32b}$$

$$\sum_{j=1}^{K} \mathbf{H}_k \mathbf{W}_j \mathbf{H}_k^H + \sigma_k^2 \geq \frac{e_k}{\eta_k \left(1-\rho_k\right)}, \tag{32c}$$

$$\mathbf{W}_k \succeq 0, \tag{32d}$$

$$0 < \rho_k < 1, \forall k \in \mathcal{K}. \tag{32e}$$

Since $\frac{1}{\rho_k}$ and $\frac{1}{1-\rho_k}$ are both convex functions with respect to ρ_k, it can be seen that the problem (P3.2) is a convex optimization problem, which can be solved by applying the CVX toolbox [44]. Next, we address the rank-one constraint. We assume that $\mathbf{W}_k^*$ and ρ_k^* are the optimal solution of the problem (P3.2). If $\mathbf{W}_k^*$ satisfies $\text{Rank}\left(\mathbf{W}_k^*\right) = 1, \forall k \in \mathcal{K}$, the optimal beamforming vector $\mathbf{w}_k^*$ of the problem (P3.1) can be obtained by eigenvalue decomposition, and the optimal PS ratios can also be expressed as ρ_k^*. If $\text{Rank}\left(\mathbf{W}_k^*\right) > 1, \forall k \in \mathcal{K}$, the optimal solutions $\mathbf{W}_k^*$ and ρ_k^* obtained by solving the problem (P3.2) are not the optimal solutions of the problem (P3). Next, we have following proposition.

Proposition 2: The optimal solution $\mathbf{W}_k^*$ of the problem (P3.2) satisfies $\text{Rank}\left(\mathbf{W}_k^*\right) = 1, \forall k \in \mathcal{K}$, i.e., the SDR for the problem (P3) is tight.

See Appendix A for the detailed proof. The joint transmit beamforming vector and PS ratio optimization (JBPO) algorithm can be summarized as **Algorithm 2**.

Algorithm 2 The **J**oint Transmit **B**eamforming vectors and **PS** Ratios **O**ptimization (JBPO) Algorithm

1: **if** $\text{Rank}\left(\mathbf{G}^H \mathbf{H}_r + \mathbf{H}_d\right) = K$ **then**
2: Solve the problem (P3.2) by applying CVX toolbox and obtain the optimal solution $\mathbf{W}_k^*$ and ρ_k^*.
3: Obtain the optimal transmit beamforming vector $\mathbf{w}_k^*$ by eigenvalue decomposition.
4: **else**
5: Exit the optimization algorithm and reinitialize.
6: **end if**
7: **return** the optimal transmit beamforming vector $\mathbf{w}^*$ and the optimal PS ratio $\boldsymbol{\rho}^*$.

C. IRS phase shift optimization

When the SIC decoding order is determined, and the beamforming vector and PS ratio are fixed, according to the variable substitution $\mathbf{u}=\left[e^{j\theta_1},...,e^{j\theta_M}\right]^H \in \mathbb{C}^{M\times 1}$ in Section III.A, the constraint on θ_m can be transformed into $|u_m|=1, \forall m \in \mathcal{M}$. Let $\mathbf{p}_{k,j}=\mathrm{diag}\left(\mathbf{h}_{r,j}^H\right)\mathbf{G}\mathbf{w}_k \in \mathbb{C}^{M\times 1}$, $\mathbf{q}_{k,j}=\mathbf{h}_{d,j}^H\mathbf{w}_k \in \mathbb{C}$. Then $\left|\left(\mathbf{h}_{r,j}^H\mathbf{\Theta}\mathbf{G}+\mathbf{h}_{d,j}^H\right)\mathbf{w}_k\right|^2=\left|\mathbf{u}^H\mathbf{p}_{k,j}+\mathbf{q}_{k,j}\right|^2$. Next we introduce auxiliary variables as follows,

$$\mathbf{S}_{k,j}=\begin{bmatrix}\mathbf{p}_{k,j}\mathbf{p}_{k,j}^H & \mathbf{p}_{k,j}\mathbf{q}_{k,j}^H\\ \mathbf{q}_{k,j}\mathbf{p}_{k,j}^H & 0\end{bmatrix}, \bar{\mathbf{u}}=\begin{bmatrix}\mathbf{u}\\ 1\end{bmatrix}, \tag{33}$$

Then $\left|\mathbf{u}^H\mathbf{p}_{k,j}+\mathbf{q}_{k,j}\right|^2=\bar{\mathbf{u}}^H\mathbf{S}_{k,j}\bar{\mathbf{u}}+|\mathbf{q}_{k,j}|^2$. Since $\bar{\mathbf{u}}^H\mathbf{S}_{k,j}\bar{\mathbf{u}}=\mathrm{Tr}\left(\mathbf{S}_{k,j}\bar{\mathbf{u}}\bar{\mathbf{u}}^H\right)$, we define $\mathbf{U}=\bar{\mathbf{u}}\bar{\mathbf{u}}^H$, where $\mathbf{U}$ satisfies $\mathbf{U}\succeq 0$ and $\mathrm{Rank}\left(\mathbf{U}\right)=1$. Since rank-one constraint is non-convex constraint, we apply the SDR to relax it. Then the problem (P1) can be transformed a feasibility-check problem (P4), which can be expressed as

$$\begin{aligned}
(\mathrm{P4}) \quad & \mathrm{find} \quad \mathbf{U} && \text{(34a)}\\
\mathrm{s.t.} \quad & \frac{\rho_k\left(\mathrm{Tr}\left(\mathbf{S}_{k,k}\mathbf{U}\right)+|\mathbf{q}_{k,k}|^2\right)}{\rho_k\sum\limits_{s(j)>s(k)}\left(\mathrm{Tr}\left(\mathbf{S}_{k,j}\mathbf{U}\right)+|\mathbf{q}_{k,j}|^2\right)+\rho_k\sigma_k^2+\delta_k^2}\geq\gamma_k, && \text{(34b)}\\
& \mathrm{Tr}\left(\mathbf{R}_{\bar{k}}\mathbf{U}\right)+\left\|\mathbf{h}_{d,\bar{k}}^H\right\|^2\geq\mathrm{Tr}\left(\mathbf{R}_k\mathbf{U}\right)+\left\|\mathbf{h}_{d,k}^H\right\|^2, \bar{k}\geq k, && \text{(34c)}\\
& \eta_k\left(1-\rho_k\right)\left(\sum_{j=1}^{K}\left(\mathrm{Tr}\left(\mathbf{S}_{k,j}\mathbf{U}\right)+|\mathbf{q}_{k,j}|^2\right)+\sigma_k^2\right)\geq e_k, && \text{(34d)}\\
& \mathbf{U}_{m,m}=1, m=1,2,...,M+1, && \text{(34e)}\\
& \mathbf{U}\succeq 0. && \text{(34f)}
\end{aligned}$$

The problem (P4) is still non-convex problem due to the fractional constraint in the constraint (34b). The problem (P4) can be transformed into the problem (P4.1), which can be expressed as the E.q. (35).

The problem (P4.1) is a standard SDP programming problem, which can be solved by CVX toolbox [44]. In general, problem (P4.1) does not produce a rank-one solution, i.e., $\mathrm{Rank}\left(\mathbf{U}\right)\neq 1$. The optimal solution obtained by the problem (P4.1) is only the upper bound of the optimal solution. Therefore, it is necessary to reconstruct the high-rank solution obtained in problem (P4.1) into a rank-one solution, that is, to reduce the rank of the high-rank solution by using

the Gaussian randomization in the subsection III.A. The IRS phase shift optimization (IPSO) algorithm can be summarized as **Algorithm 3**.

$$
\begin{aligned}
(\text{P4.1}) \quad & \text{find} \quad \mathbf{U} && \text{(35a)}\\
\text{s.t.} \quad & \tfrac{1}{\gamma_k}\left(\mathrm{Tr}\left(\mathbf{S}_{k,k}\mathbf{U}\right)+\left|\mathbf{q}_{k,k}\right|^2\right)- \\
& \sum_{s(j)>s(k)}\left(\mathrm{Tr}\left(\mathbf{S}_{k,j}\mathbf{U}\right)+\left|\mathbf{q}_{k,j}\right|^2\right)\geq \sigma_k^2+\tfrac{\delta_k^2}{\rho_k}, \ , && \text{(35b)}\\
& \mathrm{Tr}\left(\mathbf{R}_{\bar{k}}\mathbf{U}\right)+\left\|\mathbf{h}_{d,\bar{k}}^H\right\|^2\geq \mathrm{Tr}\left(\mathbf{R}_k\mathbf{U}\right)+\left\|\mathbf{h}_{d,k}^H\right\|^2, \bar{k}\geq k, && \text{(35c)}\\
& \sum_{j=1}^{K}\left(\mathrm{Tr}\left(\mathbf{S}_{k,j}\mathbf{U}\right)+\left|\mathbf{q}_{k,j}\right|^2\right)+\sigma_k^2\geq \frac{e_k}{\eta_k\left(1-\rho_k\right)}, && \text{(35d)}\\
& \mathbf{U}_{m,m}=1, m=1,2,...,M+1, && \text{(35e)}\\
& \mathbf{U}\succeq 0. && \text{(35f)}
\end{aligned}
$$

Algorithm 3 The **I**RS **P**hsae **S**hift **O**ptimization (IPSO) Algorithm

For given transmit beamforming vector $\mathbf{w}^*$ and PS ratio $\boldsymbol{\rho}^*$ according to algorithm 2, solve the SDP problem (P4.1) to obtain an optimal solution $\mathbf{U}^*$.
if $\mathrm{Rank}\left(\mathbf{U}^*\right)=1$ **then**
    Calculate the eigenvalue λ and eigenvector $\mathbf{v}$ of $\mathbf{U}^*$.
    Calculate $\boldsymbol{\Theta}^*=\mathrm{diag}\left(\sqrt{\lambda}\mathbf{v}\right)$.
else
    The eigenvalue decomposition is obtained by Eq. (25).
    for $t=1,2,...,T$ **do**
        Obtain the random vector $\mathbf{r}_t$ by using (26).
        Obatin the candidate reflection coefficients matrix $\boldsymbol{\Theta}_t$ of IRS by using Eq. (28).
    end for
    Obtain the optimal reflection coefficients matrix $\boldsymbol{\Theta}^*=\boldsymbol{\Theta}_{t^*}$ of IRS, where t^* can be obtained by using Eq. (29).
end if
return the IRS phase shift matrix $\boldsymbol{\Theta}^*$.

D. Two-stage overall optimization algorithm

Based on the previous sub-problems, we propose the two-stage optimization algorithm to minimize the BS transmit power, which is summarized as **Algorithm 4**. In the first stage, the SIC decoding order for NOMA users is determined by applying **Algorithm 1**. In the second stage, the joint transmit beamforming vector, PS ratio and IRS phase shifts are alternately optimized through **Algorithm 2** and **Algorithm 3** to achieve convergence.

Algorithm 4 Two-Stage **J**oint SIC **D**ecoding Order, Transmit **B**eamforming Vector, **P**S Ratio and I**R**S Phase Shift Optimization (JDBPR) Algorithm

1: **Stage 1:** SIC decoding order determination.
2: Obtain the SIC decoding order $\mathbf{s}$ by Algorithm 1.
3: **Stage 2:** Joint beamforming vector, PS ratio and IRS phase shift optimization.
4: Initialize $\mathbf{W}^0$, $\boldsymbol{\rho}^0$ and $\boldsymbol{\Theta}^0$. Let $r=0$, $\varepsilon=10^{-3}$.
5: **repeat**
6: According to the algorithm 2, solve the problem (P3.2) for given $\boldsymbol{\Theta}^r$, and obtain the optimal solution $\mathbf{W}^{r+1}$, $\boldsymbol{\rho}^{r+1}$.
7: According to the algorithm 3, solve the problem (P4.1) for given $\mathbf{W}^{r+1}$, $\boldsymbol{\rho}^{r+1}$, and obtain the suboptimal solution $\boldsymbol{\Theta}^{r+1}$.
8: Update $r=r+1$.
9: **until** The fractional decrease of the objective value is below a threshold ε.
10: **return** the SIC decoding order $\mathbf{s}$, transmit beamforming vector $\mathbf{W}$, PS ratio $\boldsymbol{\rho}$ and IRS phase shifts $\boldsymbol{\Theta}$.

E. Computation complexity and convergence analysis of the proposed JDBPR algorithm

1) Computation complexity analysis: Since both Algorithm 1 and Algorithm 3 optimize the IRS phase shifts, they both solve a relaxed SDP problem under different constraints, so the computational complexity of Algorithm 1 and Algorithm 3 in solving the SDP problem can be represented by $\mathcal{O}\left((M+1)^6\right)$. For the Algorithm 2, the computational complexity of using the interior point method to solve the problem (P3.2) is $\mathcal{O}\left(\sqrt{KN}\left(K^3N^2+K^2N^3\right)\right)$ [45].

2) Convergence analysis: The convergence of the proposed two-stage joint SIC decoding order, transmit beamforming vector, PS ratio and IRS phase shift optimization (JDBPR) algorithm mainly lies in the second stage because the first stage only determines the decoding order. Therefore, the convergence performance of the second-stage alternating iterative algorithm needs to be proved as follows.

We define $\mathbf{W}^r$, $\boldsymbol{\rho}^r$ and $\boldsymbol{\Theta}^r$ as the r-th iteration solution of the problem (P3.2) and (P4.1). Herein, the objective function is denoted by $\mathcal{P}\left(\mathbf{W}^r,\boldsymbol{\rho}^r,\boldsymbol{\Theta}^r\right)$. In the step 6 of Algorithm 4, since the optimal transmit beamforming vector and PS ratio can be obtained for given $\boldsymbol{\Theta}^r$. Hence, we have

$$\mathcal{P}\left(\mathbf{W}^r,\boldsymbol{\rho}^r,\boldsymbol{\Theta}^r\right)\geq\mathcal{P}\left(\mathbf{W}^{r+1},\boldsymbol{\rho}^{r+1},\boldsymbol{\Theta}^r\right). \tag{36}$$

Similarly, in the step 7 of Algorithm 4, we can obtain the sub-optimal reflection coefficients when $\mathbf{W}^{r+1}$ and $\boldsymbol{\rho}^{r+1}$ are given. Herein, we also have

$$\mathcal{P}\left(\mathbf{W}^{r+1},\boldsymbol{\rho}^{r+1},\boldsymbol{\Theta}^r\right)\geq\mathcal{P}\left(\mathbf{W}^{r+1},\boldsymbol{\rho}^{r+1},\boldsymbol{\Theta}^{r+1}\right). \tag{37}$$

Based on the above, we can obtain

$$\mathcal{P}\left(\mathbf{W}^{r}, \boldsymbol{\rho}^{r}, \boldsymbol{\Theta}^{r}\right) \geq \mathcal{P}\left(\mathbf{W}^{r+1}, \boldsymbol{\rho}^{r+1}, \boldsymbol{\Theta}^{r+1}\right), \tag{38}$$

which shows that the value of the objective function is non-increasing after each iteration in the second stage of Algorithm 4. Since the objective function values of problems (P3.2) and (P4.1) have a finite lower bound, the convergence of Algorithm 4 can be guaranteed.

IV. Numerical results

In this section, we provide simulation results to demonstrate the effectiveness of the proposed JDBPR algorithm in IRS-assisted SWIPT NOMA networks through numerical simulation. In this paper, we consider a three-dimensional (3D) coordinate system, where the BS and the IRS placed on the building are located at (0m, 0m, 15m) and (50m, 50m, 15m), respectively, and $K = 4$ ground users are randomly and uniformly distributed in a circle whose origin is (0m, 0m, 0m) and a radius of 200m. We consider that the BS is equipped with $N = 4$ antennas, and the IRS is equipped with 30 reflecting elements. We assume that the parameters of all users are the same, i.e., $\sigma_k^2 = \sigma^2$, $\delta_k^2 = \delta^2$, $\eta_k = \eta$, $\gamma_k = \gamma$ and $e_k = e$. Herein, we set $\sigma^2 = -70$dBm, $\delta^2 = -50$dBm and $\eta = 0.7$ in our numerical simulations. The path loss exponents are set as $\alpha = 3$, $\beta = 2.2$ and $o = 2.5$. We set the path loss C_0 to -30dB when the reference distance is 1m, and we set the Rician factor κ to 3dB. The convergence threshold of the JDBPR algorithm is set as 10^{-3}.

We first evaluate the convergence performance of the proposed JDBPR algorithm. Fig. 3 shows the BS transmit power varies with the number of iterations under different IRS reflecting elements. It can be seen that as the number of iterations increases, the BS transmit power gradually decreases. The algorithm can reach convergence in the 7-th iteration, which verifies that the proposed algorithm converges fast. Specifically, we compare the performance of the JDBPR algorithm when the number of IRS reflecting elements are 30, 60, and 80 respectively. It can be seen that the greater the number of IRS reflecting elements, the lower the BS transmit power, which also verifies the effectiveness of the IRS assisted SWIPT NOMA networks.

Next, we compare the performance of the proposed JDBPR algorithm with other baseline algorithms. (1) EX-JBPR-opt algorithm: The users' decoding order adopts the exhaustive search method. The optimization of beamforming vector and PS ratio adopts JBPO algorithm, and the optimization of IRS phase shifts adopts IPSO algorithm. It is called the EX-JBPR-opt

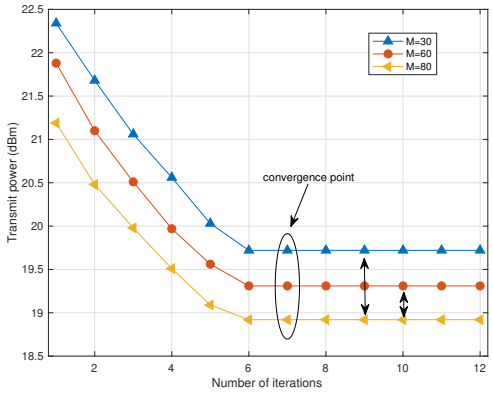

Fig. 3. The convergence of the proposed JDBPR algorithm.

algorithm. (2) TS-JDBPR-opt algorithm: The proposed two-stage JDBPR algorithm, i.e., TS-JDBPR-opt algorithm. (3) TS-JDBPR-com algorithm: The algorithm is divided into two stages. The SIC decoding order in the first stage adopts the proposed SDOD algorithm. In the second stage, the optimization of the beamforming vector and PS ratio adopts the JBPO algorithm, and optimization of IRS phase shifts adopts the IPSO algorithm. Different from the TS-JDBPR-opt algorithm, the two sub-problems in the second stage are not optimized alternately. (4) TS-JDBPR-ZF algorithm: The only difference from the TS-JDBPR-opt algorithm is that the design of the beamforming vector uses the sub-optimal ZF beamforming scheme, which can eliminate user interference [14]. (5) TS-JDBR-ran algorithm: The only difference from the TS-JDBPR-opt algorithm is that the design of IRS phase shifts adopts a random scheme.

Herein, we investigate the behavior of the BS transmit power with the QoS requirements of all users under different energy harvested threshold e. Fig. 4 and Fig. 5 respectively show how the BS transmit power varies with the users' QoS requirements under different energy harvested threshold (e.g. $e = 0$dBm and $e = -10$dBm). From Fig. 4 and Fig. 5, we can see that the BS transmit power under different algorithms increases with the increase of users' QoS threshold. This is because the larger the users' QoS threshold, the higher the requirements for the BS transmit power. In addition, it can be seen that the performance of the proposed TS-JDBPR-opt algorithm is similar to the EX-JBPR-opt algorithm, but the complexity of exhaustive search is much higher than the SDOD algorithm. At the same time, our proposed TS-JDBPR-opt algorithm has better performance than the other three baseline algorithms. In specific analysis, the better performance of the TS-JDBPR-opt algorithm compared to the TS-JDBPR-com algorithm

is mainly because the former is considered from the perspective of global optimization, while the latter only performs local optimization. Compared with the TS-JDPR-ZF algorithm, our proposed beamforming scheme at the BS has better performance. This is because that the ZF beamforming scheme is a sub-optimal scheme. The TS-JDBR-ran algorithm designs the IRS reflection coefficient matrix in a random manner, so the solution to our proposed algorithm has a better performance.

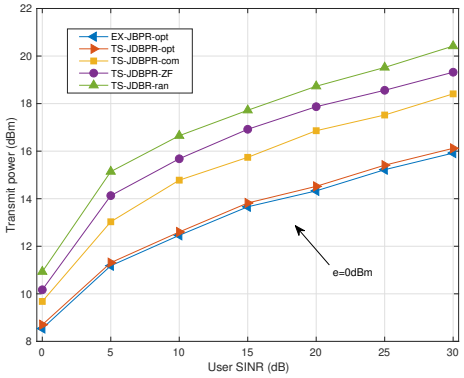

Fig. 4. The BS transmit power versus QoS threshold when $e = 0$dBm.

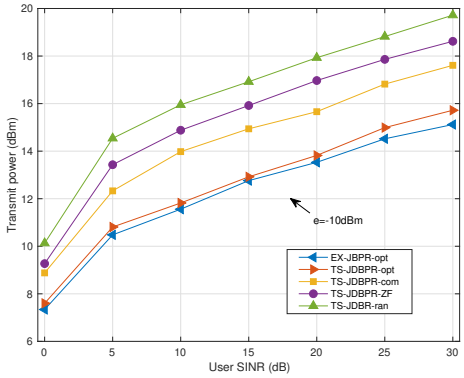

Fig. 5. The BS transmit power versus QoS threshold when $e = -10$dBm.

Fig. 6 and Fig. 7 elaborate how the BS transmit power varies with the user's energy harvested threshold under different users' QoS threshold (e.g. γ = 10dB and γ = 0dB). In general, as the user energy harvested threshold increases, the transmit power required by the BS continues to increase. This is mainly because the increase in the energy harvested threshold required by the user will require the BS to give a stronger transmission signal. When we consider that the users' QoS threshold is 10dB, it can be seen that the proposed TS-JDBPR-opt algorithm requires similar transmit power to the EX-JBPR-opt algorithm, but its complexity is much lower than the latter. This is mainly because the latter adopts the exhaustive search method in the decoding order scheme, which is more complicated. In addition, the performance of the TS-JDBPR-opt algorithm is also better than the other three baseline algorithms. The reason why the TS-JDBPR-opt algorithm performs better than the TS-JDBPR-com algorithm is that the latter does not achieve the convergence of the entire problem. Compared with the TS-JDBR-ran algorithm, the TS-JDBPR-opt algorithm can greatly reduce the BS transmit power, because that the TS-JDBR-ran algorithm does not optimize the reflection coefficients matrix of the IRS, and the random phase may even make the system performance worse. In addition, when the users'

QoS threshold is 0dB, the change of the BS transmit power with the user's energy harvested threshold is similar to the former. Meanwhile, comparing Fig. 6 and Fig. 7, we can also see that when the user's energy harvested threshold is the same, the higher the users' QoS threshold, the greater the transmission power required by the BS.

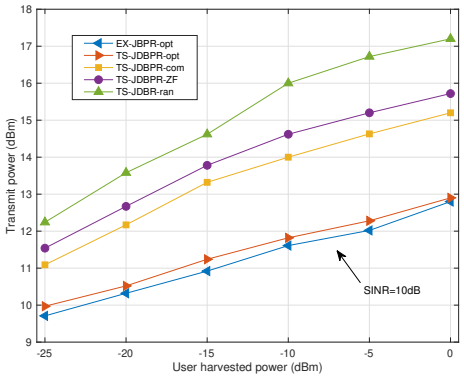

Fig. 6. The BS transmit power versus harvested power when γ = 10dB.

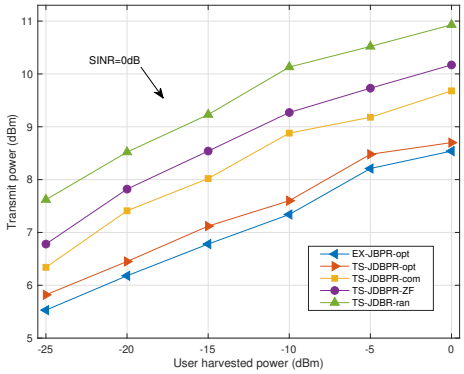

Fig. 7. The BS transmit power versus harvested power when γ = 0dB.

Fig. 8 illustrates the variation of BS transmit power with the number of IRS reflecting elements under different algorithms. In general, it can be seen that as the number of reflecting elements of the IRS increases, the BS transmit power continues to decrease. This is because that the channel can be adjusted through the IRS, so that the system performance is enhanced, that is, the BS transmit power is gradually reduced. From Fig. 8, it can be seen that the performance of SWIPT NOMA networks with IRS assistance is better than the networks without IRS assistance. Furthermore, when the reflecting elements of IRS increase, the gap of this performance becomes larger, which also verifies that IRS has a very important auxiliary role in SWIPT NOMA networks. At the same time, our proposed TS-JDBPR-opt algorithm achieves a significant performance improvement compared to the TS-JDBPR-com algorithm and the TS-JDBR-ran algorithm. The main reason is that the TS-JDBPR-com algorithm does not achieve global convergence, and the TS-JDBR-ran algorithm does not optimize the IRS phase shifts. Fig. 8 can also demonstrate that we can reduce the transmit power on the BS by increasing the number of IRS reflecting elements, and the cost of this scheme is very low.

Finally, Fig. 9 explains how the BS transmit power versus the number of BS antennas under different algorithms. With the increase of the number of antennas, the BS transmit power continues to decrease, which also shows that we can improve the performance of the system by

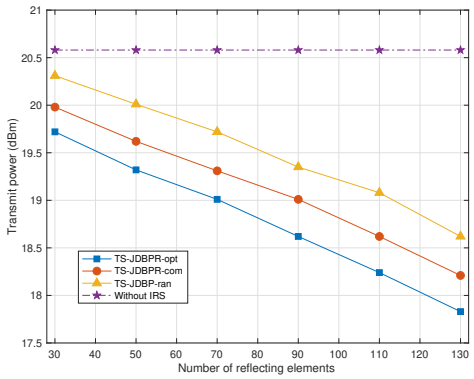

Fig. 8. The BS transmit power versus number of reflecting elements M.

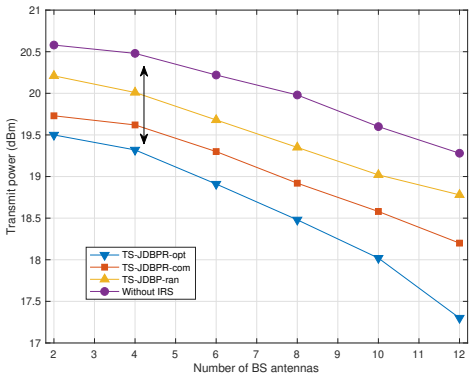

Fig. 9. The BS transmit power versus number of BS antennas N.

increasing the number of BS antennas. This also motivates us to adopt massive MIMO systems to further enhance the IRS-assisted SWIPT NOMA networks. In addition, when the number of antennas is the same, the proposed TS-JDBPR-opt algorithm still yields a significant performance improvement compared to the TS-JDBPR-com algorithm and the TS-JDBR-ran algorithm.

V. Conclusion

This paper investigates the transmit power minimization problem for the IRS-assisted SWIPT NOMA networks. Specifically, under the users' QoS and energy harvesting constraints, the SIC decoding order, the BS transmit beamforming vector, the PS ratio, and the IRS phase shift matrix are jointly optimized. The feasibility conditions of the problem are first derived and demonstrated. Then, this challenging problem is is solved by a two-stage algorithm. In the first stage, an SIC decoding order determination algorithm based on the combined channel strength has been proposed. Further, we divide the second stage into two sub-problems. First, the BS transmit beamforming and the received PS ratio are optimized by applying SDR, which is then proved to be tight. Second, the IRS phase shift matrix are optimized by SDR and Gaussian randomization. Then, the two sub-problems are optimized alternately until convergence is achieved. In addition, the computation complexity and convergence of the proposed optimization algorithm are analyzed and proved, that is, the computational complexity of the proposed algorithm is much lower than that of the exhaustive search method but has similar performance, and the algorithm converges fast with different simulation parameters. Numerical results show that our proposed algorithm can significantly reduce the BS transmit power compared to other baseline algorithms, and the

auxiliary role of IRS is extremely important, which can greatly relieve the pressure on the BS with low cost in practice.

APPENDIX A
PROOF OF THE PROPOSITION 2

Since the problem (P3) is a convex optimzation problem and satisfies the Slater's condition, the duality gap is zero. Let $\mathbf{\Psi}_k \in \mathbb{C}^{N\times N}$, ς_k and ε_k denote the dual variables related to $\mathbf{W}_k$, QoS requirements constraint and energy harvested constraint in the problem (P3.1), the Lagrangian function of problem (P3.1) can be expressed as

$$\begin{aligned}
&\mathcal{L}\left(\mathbf{W}_k, \rho_k, \mathbf{\Psi}_k, \varsigma_k, \varepsilon_k\right) = \sum_{k=1}^{K} \mathrm{Tr}\left(\mathbf{W}_k\right) - \sum_{k=1}^{K} \mathrm{Tr}\left(\mathbf{\Psi}_k \mathbf{W}_k\right) \\
&- \sum_{k=1}^{K} \varsigma_k \left(\frac{\mathbf{H}_k \mathbf{W}_k \mathbf{H}_k^H}{\gamma_k} - \sum_{s(j)>s(k)} \mathbf{H}_k \mathbf{W}_j \mathbf{H}_k^H - \sigma_k^2 - \frac{\delta_k^2}{\rho_k} \right) \\
&- \sum_{k=1}^{K} \varepsilon_k \left(\sum_{j=1}^{K} \mathbf{H}_k \mathbf{W}_j \mathbf{H}_k^H + \sigma_k^2 - \frac{e_k}{\eta_k\left(1-\rho_k\right)} \right) = \mathbf{\Gamma} - \\
&\sum_{k=1}^{K} \mathrm{Tr}\left(\mathbf{\Psi}_k \mathbf{W}_k\right) + \sum_{k=1}^{K} \left(\varsigma_k - \varepsilon_k\right)\sigma_k^2 + \sum_{k=1}^{K} \left(\frac{\varsigma_k \delta_k^2}{\rho_k} + \frac{\varepsilon_k e_k}{\eta_k\left(1-\rho_k\right)} \right),
\end{aligned} \tag{39}$$

where $\mathbf{\Gamma} = \sum_{k=1}^{K} \mathrm{Tr}\left(\mathbf{W}_k\right) - \sum_{k=1}^{K} \varsigma_k \left(\frac{\mathbf{H}_k \mathbf{W}_k \mathbf{H}_k^H}{\gamma_k} - \sum_{s(j)>s(k)} \mathbf{H}_k \mathbf{W}_j \mathbf{H}_k^H \right) - \sum_{k=1}^{K} \varepsilon_k \left(\sum_{j=1}^{K} \mathbf{H}_k \mathbf{W}_j \mathbf{H}_k^H \right)$. Therefore, the dual problem of the problem (P3.1) can be given by

$$\min_{0<\rho_k<1, \forall k \in \mathcal{K},} \mathcal{L}\left(\mathbf{W}_k, \rho_k, \mathbf{\Psi}_k, \varsigma_k, \varepsilon_k\right), \tag{40}$$

The optimal solution can be expressed as

$$\max_{\substack{\mathbf{\Psi}_k 0, \varsigma_k, \varepsilon_k \geq 0, \\ \forall k \in \mathcal{K},}} \min_{\substack{\mathbf{W}_k \succeq 0, 0<\rho_k<1, \\ \forall k \in \mathcal{K},}} \mathcal{L}\left(\mathbf{W}_k, \rho_k, \mathbf{\Psi}_k, \varsigma_k, \varepsilon_k\right). \tag{41}$$

Then, we observe the structure of the optimal solution $\mathbf{W}_k^*$ of the dual problem through the Karush-Kuhn-Tucker (KKT) condition. The optimal solution related to $\mathbf{W}_k^*$ satisfies the following conditions:

$$\mathrm{K1}: \varsigma_k^*, \varepsilon_k^* \geq 0, \mathbf{\Psi}_k^* \succeq 0; \mathrm{K2}: \mathbf{\Psi}_k^* \mathbf{W}_k^* = 0; \mathrm{K3}: \nabla_{\mathbf{W}_k^*} \mathcal{L} = 0. \tag{42}$$

For K3, we rewrite it as follows,

$$\mathbf{\Psi}_k^* = \mathbf{I}_N - \left(\frac{\varsigma_k^*}{\gamma_k} + \varepsilon_k^*\right)\mathbf{H}_k^H\mathbf{H}_k \triangleq \mathbf{I}_N - \mathbf{\Lambda}. \tag{43}$$

We verify that the optimal beamforming matrix must be a rank-one matrix by observing the structure of $\mathbf{\Psi}_k^*$. According to $\mathrm{Rank}\,(\mathrm{A}) + \mathrm{Rank}\,(\mathrm{B}) \geq \mathrm{Rank}\,(\mathrm{A}+\mathrm{B})$, $\mathrm{Rank}\,(\mathbf{\Psi}_k^*) \geq N - 1$ can be derived. When $\mathrm{Rank}\,(\mathbf{\Psi}_k^*) = N$, according to K2 of the KKT condition, we can obtain $\mathrm{Rank}\,(\mathbf{W}_k^*) = 0$. Then $\mathbf{W}_k^* = \mathbf{0}$, which cannot be the optimal solution to the problem (P3.1). Therefore, $\mathrm{Rank}\,(\mathbf{\Psi}_k^*) = N - 1$, we can obtain $\mathrm{Rank}\,(\mathbf{W}_k^*) = 1$. Rank-one certificate is completed. In addition, the optimal PS ratios satisfy the following problem

$$\min \quad \frac{\varsigma_k^*\delta_k^2}{\rho_k} + \frac{\varepsilon_k^* e_k}{\eta_k\left(1-\rho_k\right)}, \tag{44a}$$

$$\text{s.t.} \qquad 0 < \rho_k < 1, \forall k \in \mathcal{K}. \tag{44b}$$

Based on the above content, two conclusions can be drawn as follows,

(1) If $\varsigma_k^* = 0$, $\varepsilon_k^* = 1$, the optimal $\rho_k^* \to 0$; (2) If $\varsigma_k^* = 1$, $\varepsilon_k^* = 0$, the optimal $\rho_k^* \to 1$.

Taking into account $\gamma_k > 0, e_k > 0$ in the problem (P3.1), i.e., $0 < \rho_k^* < 1, \forall k \in \mathcal{K}$, the above two cases will not happen. According to KKT condition K1, $\varsigma_k^* > 0, \varepsilon_k^* > 0$ can be obtained. Combining with the complementary relaxation [46], it can be obtained the equal sign for the QoS requirements constraint and the energy harvested constraint.

REFERENCES

[1] Q. Wu and R. Zhang, "Towards smart and reconfigurable environment: Intelligent reflecting surface aided wireless network," *IEEE Commun. Mag.*, vol. 58, no. 1, pp. 106–112, 2020.

[2] W. Ni, X. Liu, Y. Liu, H. Tian, and Y. Chen, "Resource allocation for multi-cell IRS-aided NOMA networks," *arXiv preprint arXiv:2006.11811*, 2020.

[3] L. Lu, G. Y. Li, A. L. Swindlehurst, A. Ashikhmin, and R. Zhang, "An overview of massive MIMO: Benefits and challenges," *IEEE J. Sel. Topics Signal Process.*, vol. 8, no. 5, pp. 742–758, 2014.

[4] Q. Wu, W. Chen, M. Tao, J. Li, H. Tang, and J. Wu, "Resource allocation for joint transmitter and receiver energy efficiency maximization in downlink OFDMA systems," *IEEE Trans. Commun.*, vol. 63, no. 2, pp. 416–430, 2015.

[5] Y. Liu, Z. Qin, M. Elkashlan, Z. Ding, A. Nallanathan, and L. Hanzo, "Non-orthogonal multiple access for 5G and beyond," *Proc. IEEE*, vol. 105, no. 12, pp. 2347–2381, 2017.

[6] L. Dai, B. Wang, Y. Yuan, S. Han, I. Chih-lin, and Z. Wang, "Non-orthogonal multiple access for 5g: solutions, challenges, opportunities, and future research trends," *IEEE Commun. Mag.*, vol. 53, no. 9, pp. 74–81, 2015.

[7] Y. Zhou, V. W. S. Wong, and R. Schober, "Coverage and rate analysis of millimeter wave NOMA networks with beam misalignment," *IEEE Trans. Wireless Commun.*, vol. 17, no. 12, pp. 8211–8227, 2018.

[8] F. Wei and W. Chen, "Low complexity iterative receiver design for sparse code multiple access," *IEEE Trans. Commun.*, vol. 65, no. 2, pp. 621–634, 2017.

[9] Y. Cai, Z. Qin, F. Cui, G. Y. Li, and J. A. McCann, "Modulation and multiple access for 5G networks," *IEEE Communications Surveys Tutorials*, vol. 20, no. 1, pp. 629–646, 2018.

[10] Z. Ding, Y. Liu, J. Choi, Q. Sun, M. Elkashlan, I. Chih-Lin, and H. V. Poor, "Application of non-orthogonal multiple access in LTE and 5G networks," *IEEE Commun. Mag.*, vol. 55, no. 2, pp. 185–191, 2017.

[11] Z. Ding, P. Fan, and H. V. Poor, "Impact of user pairing on 5G nonorthogonal multiple-access downlink transmissions," *IEEE Trans. Veh. Technol.*, vol. 65, no. 8, pp. 6010–6023, 2016.

[12] Y. Zeng, B. Clerckx, and R. Zhang, "Communications and signals design for wireless power transmission," *IEEE Trans. Commun.*, vol. 65, no. 5, pp. 2264–2290, 2017.

[13] B. Clerckx, R. Zhang, R. Schober, D. W. K. Ng, D. I. Kim, and H. V. Poor, "Fundamentals of wireless information and power transfer: From RF energy harvester models to signal and system designs," *IEEE J. Sel. Areas Commun.*, vol. 37, no. 1, pp. 4–33, 2019.

[14] Q. Shi, L. Liu, W. Xu, and R. Zhang, "Joint transmit beamforming and receive power splitting for MISO SWIPT systems," *IEEE Trans. Wireless Commun.*, vol. 13, no. 6, pp. 3269–3280, 2014.

[15] X. Zhou, R. Zhang, and C. K. Ho, "Wireless information and power transfer: Architecture design and rate-energy tradeoff," *IEEE Trans. Commun.*, vol. 61, no. 11, pp. 4754–4767, 2013.

[16] Q. Wu and R. Zhang, "Intelligent reflecting surface enhanced wireless network via joint active and passive beamforming," *IEEE Trans. Wireless Commun.*, vol. 18, no. 11, pp. 5394–5409, 2019.

[17] Q. Wu and R. Zhang, "Beamforming optimization for wireless network aided by intelligent reflecting surface with discrete phase shifts," *IEEE Trans. Commun.*, vol. 68, no. 3, pp. 1838–1851, 2020.

[18] W. Tang, M. Z. Chen, J. Y. Dai, Y. Zeng, X. Zhao, S. Jin, Q. Cheng, and T. J. Cui, "Wireless communications with programmable metasurface: New paradigms, opportunities, and challenges on transceiver design," *IEEE Wireless Commun.*, vol. 27, no. 2, pp. 180–187, 2020.

[19] C. Huang, S. Hu, G. C. Alexandropoulos, A. Zappone, C. Yuen, R. Zhang, M. D. Renzo, and M. Debbah, "Holographic MIMO surfaces for 6G wireless networks: Opportunities, challenges, and trends," *IEEE Wireless Commun.*, vol. 27, no. 5, pp. 118–125, 2020.

[20] X. Yuan, Y.-J. Zhang, Y. Shi, W. Yan, and H. Liu, "Reconfigurable-intelligent-surface empowered 6G wireless communications: Challenges and opportunities," *arXiv preprint arXiv:2001.00364*, 2020.

[21] C. Liaskos, S. Nie, A. Tsioliaridou, A. Pitsillides, S. Ioannidis, and I. Akyildiz, "A new wireless communication paradigm through software-controlled metasurfaces," *IEEE Commun. Mag.*, vol. 56, no. 9, pp. 162–169, 2018.

[22] N. Rajatheva, I. Atzeni, E. Bjornson, A. Bourdoux, S. Buzzi, J.-B. Dore, S. Erkucuk, M. Fuentes, K. Guan, Y. Hu *et al.*, "White paper on broadband connectivity in 6G," *arXiv preprint arXiv:2004.14247*, 2020.

[23] S. Gong, X. Lu, D. T. Hoang, D. Niyato, L. Shu, D. I. Kim, and Y.-C. Liang, "Towards smart radio environment for wireless communications via intelligent reflecting surfaces: A comprehensive survey," *arXiv preprint arXiv:1912.07794*, 2019.

[24] J. Zhao, "A survey of intelligent reflecting surfaces (IRSs): Towards 6G wireless communication networks with massive MIMO 2.0," *arXiv preprint arXiv:1907.04789*, 2019.

[25] W. Yan, X. Yuan, Z. Q. He, and X. Kuai, "Passive beamforming and information transfer design for reconfigurable intelligent surfaces aided multiuser MIMO systems," *IEEE J. Sel. Areas Commun.*, vol. 38, no. 8, pp. 1793–1808, 2020.

[26] L. Dong and H. Wang, "Enhancing secure MIMO transmission via intelligent reflecting surface," *IEEE Trans. Wireless Commun.*, pp. 1–1, 2020.

[27] S. Hong, C. Pan, H. Ren, K. Wang, and A. Nallanathan, "Artificial-noise-aided secure MIMO wireless communications via intelligent reflecting surface," *IEEE Trans. Commun.*, pp. 1–1, 2020.

[28] T. Bai, C. Pan, Y. Deng, M. Elkashlan, A. Nallanathan, and L. Hanzo, "Latency minimization for intelligent reflecting surface aided mobile edge computing," *IEEE J. Sel. Areas Commun.*, vol. 38, no. 11, pp. 2666–2682, 2020.

[29] T. Shafique, H. Tabassum, and E. Hossain, "Optimization of wireless relaying with flexible UAV-borne reflecting surfaces," *IEEE Trans. Commun.*, pp. 1–1, 2020.

[30] S. Li, B. Duo, X. Yuan, Y. Liang, and M. Di Renzo, "Reconfigurable intelligent surface assisted UAV communication: Joint trajectory design and passive beamforming," *IEEE Wireless Commun. Lett.*, vol. 9, no. 5, pp. 716–720, 2020.

[31] H. Shen, W. Xu, S. Gong, Z. He, and C. Zhao, "Secrecy rate maximization for intelligent reflecting surface assisted Multi-antenna communications," *IEEE Commun. Lett.*, vol. 23, no. 9, pp. 1488–1492, 2019.

[32] L. Lv, Q. Wu, Z. Li, N. Al-Dhahir, and J. Chen, "Secure two-way communications via intelligent reflecting surfaces," *IEEE Commun. Lett.*, pp. 1–1, 2020.

[33] M. Fu, Y. Zhou, Y. Shi, and K. B. Letaief, "Reconfigurable intelligent surface empowered downlink non-orthogonal multiple access," *arXiv preprint arXiv:1910.07361*, 2019.

[34] B. Zheng, Q. Wu, and R. Zhang, "Intelligent reflecting surface-assisted multiple access with user pairing: NOMA or OMA?" *IEEE Commun. Lett.*, vol. 24, no. 4, pp. 753–757, 2020.

[35] J. Zuo, Y. Liu, Z. Qin, and N. Al-Dhahir, "Resource allocation in intelligent reflecting surface assisted NOMA systems," *IEEE Trans. Commun.*, pp. 1–1, 2020.

[36] M. Zeng, X. Li, G. Li, W. Hao, and O. A. Dobre, "Sum rate maximization for IRS-assisted uplink NOMA," *IEEE Commun. Lett.*, pp. 1–1, 2020.

[37] J. Zuo, Y. Liu, E. Basar, and O. A. Dobre, "Intelligent reflecting surface enhanced millimeter-wave NOMA systems," *IEEE Commun. Lett.*, pp. 1–1, 2020.

[38] J. Zhu, Y. Huang, J. Wang, K. Navaie, and Z. Ding, "Power efficient IRS-assisted NOMA," *IEEE Trans. Commun.*, pp. 1–1, 2020.

[39] Q. Wu and R. Zhang, "Weighted sum power maximization for intelligent reflecting surface aided SWIPT," *IEEE Wireless Commun. Lett.*, vol. 9, no. 5, pp. 586–590, 2020.

[40] Q. Wu and R. Zhang, "Joint active and passive beamforming optimization for intelligent reflecting surface assisted SWIPT under QoS constraints," *IEEE J. Sel. Areas Commun.*, vol. 38, no. 8, pp. 1735–1748, 2020.

[41] C. Pan, H. Ren, K. Wang, M. Elkashlan, A. Nallanathan, J. Wang, and L. Hanzo, "Intelligent reflecting surface aided MIMO broadcasting for simultaneous wireless information and power transfer," *IEEE J. Sel. Areas Commun.*, vol. 38, no. 8, pp. 1719–1734, 2020.

[42] L. Subrt and P. Pechac, "Intelligent walls as autonomous parts of smart indoor environments," *IET Commun.*, vol. 6, no. 8, pp. 1004–1010, 2012.

[43] J. Cui, Y. Liu, Z. Ding, P. Fan, and A. Nallanathan, "Optimal user scheduling and power allocation for millimeter wave NOMA systems," *IEEE Trans. Wireless Commun.*, vol. 17, no. 3, pp. 1502–1517, 2018.

[44] M. Grant and S. Boyd, "CVX: Matlab software for disciplined convex programming, version 2.1," 2014.

[45] A. Ben-Tal and A. Nemirovski, *Lectures on modern convex optimization: analysis, algorithms, and engineering applications*. SIAM, 2001.

[46] S. Boyd, S. P. Boyd, and L. Vandenberghe, *Convex optimization*. Cambridge university press, 2004.